

Task-based Compliance Control for Bottle Screw Manipulation with a Dual-arm Robot

Chunting Jiao, Lin Zhang, Xiaojie Su, Jiangshuai Huang, Zhenshan Bing, and Alois Knoll

Abstract—In this paper, a novel task-based compliance control approach for a dual-arm robot is presented with a bottle screw task. The presented approach aims at overcoming uncertainties from the object model and contact forces during the bottle screw task. A novel framework is proposed to synthesize the task motion planning and compliance control that ensure desired performance of both accuracy and compliant motion. The proposed task-based compliance control approach provides a hierarchical strategy: gross motion planning and fine compliance motion planning. The gross motion planning involves the absolute and relative motion control on a macro scale, while the fine compliance motion planning deals with uncertainties by the compliance control to accomplish a task requiring high precision robustly. A theoretical modeling of the bottle screw task is presented within the proposed framework through the analysis of uncertainties and constraints. The experimental results show that the proposed framework is efficient and robust to operate a set of bottles.

Index Terms—Dual-arm manipulation, task-based control, gross motion, fine motion, hybrid control, bottle manipulation

I. Introduction

Bottle screw task is one of the most common daily-life tasks, it is yet to be discussed widely. In previous studies, some researchers focused only on opening a jar, a can or a bottle. Both Honda's Asimo anthropomorphic robot and Stanford University's PR2 robot attempted the task of opening a bottle cap. But they did not fasten it back, which reduced the complexity of the experiment. One of the challenges for this task is the absence of a widely-accepted framework that combines the motion planning and compliance control to guarantee the stability of both accuracy motion and contact forces [1]. In particular, kinematic and contact uncertainties are inevitable and may lead to the failure of the task [2].

The bottle screw task is similar to precision peg-in-hole assembly, in which both the accurate position control and

compliance force control are required [3], [4]. Traditionally, the robotic peg-in-hole assembly task is divided into two phases, i.e, the alignment phase and the insertion phase [5], [6]. Visual servo control and pose estimation are applied in the alignment phase, and force guided assembly is used in the insertion phase. The clearance between the bottle cap and body is only about 1 mm, making it difficult for the cap to fit accurately on the top of the bottle. Thus, similar to the robotic peg-in-hole assembly task, the execution process of the bottle screw task in daily life can be divided into four stages: grasping the bottle, opening the bottle cap, pouring water and screwing on the bottle cap. The accuracy position control is used to match the bottle cap and body, and the compliance force control is required to compensate for the positional uncertainty. Moreover, the force feedback can be applied to detect the contact state to prevent stuck.

The main academic control problem in the bottle screw task lies in the uncertainties, which can be classified into two categories [7]:

- 1) The kinematic model of the robot and object is uncertain, including both the geometric and motion uncertainties;
- 2) The contact state is uncertain. During the dynamic manipulation, the interaction force may cause an unexpected relative movement between the bottle and the gripper, resulting in an unstable grasp.

The uncertainties are likely to make the task fail, for example, if the cap and the edge of the bottle collide, the cap cannot be placed on the bottle or the cap may get stuck due to the uneven force during the screw motion. To overcome these uncertainties, several approaches for a dual-arm manipulation have been proposed in the previous studies [8], [9], [10]. Visual recognition is used to reduce the positional uncertainty. Motion planning method is discussed to find an available joint sequence between the start and goal. A couple of hybrid position/force control methods have been studied thoroughly. Hyeonjun proposed a compliance-based method by analyzing the contact state without any force feedback [8]. Jiao et al. [9] presented an adaptive hybrid impedance control method for dual-arm cooperative manipulation with object uncertainties. In [10], the Markov decision process of the assembly task was formulated, where the task was accomplished through the learned policy without analyzing the contact state. On the other hand, the active compliant control was talked about in [11], [12].

This work was partially supported by the National Key Research and Development Program of China (2022YFE0107300), the National Natural Science Foundation of China (U22A20101 62003061, 62173051), the Chongqing Technology Innovation and Application Development Special Key Project (CSTB2022TIAD-CUX0015 CSTB2022TIAD-KPX0162), and the Postdoctoral Science Foundation of China (2021M700591). (Corresponding author: Xiaojie Su)

Chunting Jiao, Lin Zhang, Xiaojie Su, and Jiangshuai Huang are with the Department of Automation, Chongqing University, Chongqing, 400044, China (chtjiao@cqu.edu.cn, lin.zhang@cqu.edu.cn, suxiaojie@cqu.edu.cn, jshuang@cqu.edu.cn).

Zhenshan Bing and Alois Knoll are with the Department of Informatics, Technical University of Munich, Munich, 80333, Germany (bing@in.tum.de, knoll@in.tum.de).

The contact force errors were compensated by Cartesian impedance control. Ren introduced a novel autonomous assembly application completed by a dual-arm robot by using a hybrid position/force control [13]. Event-triggered sliding mode control methods were proposed in [14], [15] to study the system and parameter uncertainties. Adaptive neural tracking control methods for manipulators are discussed in [16], [17], [18], [19] for trajectory tracking of robotic systems.

The main contributions of the present work can be summarized as follows:

- 1) A novel task-based manipulation planning framework is proposed for a dual-arm robotic system. This framework imitates human behavior and can improve the efficiency and robustness of task execution;
- 2) An active compliant motion method is characterized by force-based feedback control to tackle contact state uncertainties;
- 3) A theoretical model of the bottle screw task is constructed, which can be extended to screw-tightening task.

II. Cooperative Task Space

Inspired by human behaviors, we can roughly partition the task space of a robot into absolute and relative motion components [20]. The absolute motion is performed by the master arm, which is aimed to achieve the accurate and robust tracking of the reference trajectories. The relative task can be conducted by the slave arm, which is described solely through a relative motion of the robot's end-effectors, i.e., the motion of one end-effector with respect to the other.

A. Task Formulation for Coordinated Motion

Consider a robot system composed by two arms, as shown in Fig. 1, which are denoted by Arm- k , where $k = a, b$. The reference frames are defined as follows: Σ_{world} is the world frame, Σ_{ok} is the base frame of Arm- k , and Σ_{ek} is the end-effector frame of Arm- k . The world frame Σ_{world} is set as the default reference frame. Let $p_{ek} \in R^3$ denotes the position vector of the end-effector of Arm- k and $R_{ek} \in SO(3)$ is the rotation matrix of the end-effector orientation of Arm- k with respect to the base frame Σ_{ok} . We write the angle-axis representation of R_{ek} as $R_j(v_{ek})$, where v_{ek} is the angle through which one must rotate about the axis j to obtain R_{ek} . $T_{ek} = (R_{ek}, p_{ek}) \in SE(3)$ denotes the homogeneous transformation matrix of the end-effector, where $x_{ek} = (x, y, z, \alpha, \beta, \gamma)^T$ is the corresponding pose (position and orientation) of the end-effector. The orientation of the end-effector is represented by the Z - Y - X Euler angles. $\dot{p}_{ek} \in R^3$ and $\omega_{ek} \in R^3$ represent, respectively, the linear and angular velocities of the k -th end-effector, which can be collected in the generalized velocity vector $v_{ek} = (\dot{p}_{ek}^T, \omega_{ek}^T)^T \in R^6$. $q \in C$ is the joint state in the configuration space $C \subset R^6$, and \dot{q}_a and \dot{q}_b are the joint angular velocities of the two arms.

Besides this, the real-time force and torque information F_{ek} is described in the end-effector frame Σ_{ek} , which can be used to guide the motion of the robot arms. Then, the differential forward kinematics can be expressed as:

$$\begin{cases} v_{ea} = J_a(q_a) \dot{q}_a \\ v_{eb} = J_b(q_b) \dot{q}_b \end{cases} \quad (1)$$

where the matrix $J_k \in R^{6 \times 6}$ is the so-called geometric Jacobian of the Arm- k . Without the loss of generality, assume the Arm- a as the master arm which is used to generate the absolute motion, and the Arm- b as the slave arm, as shown in Fig. 1.

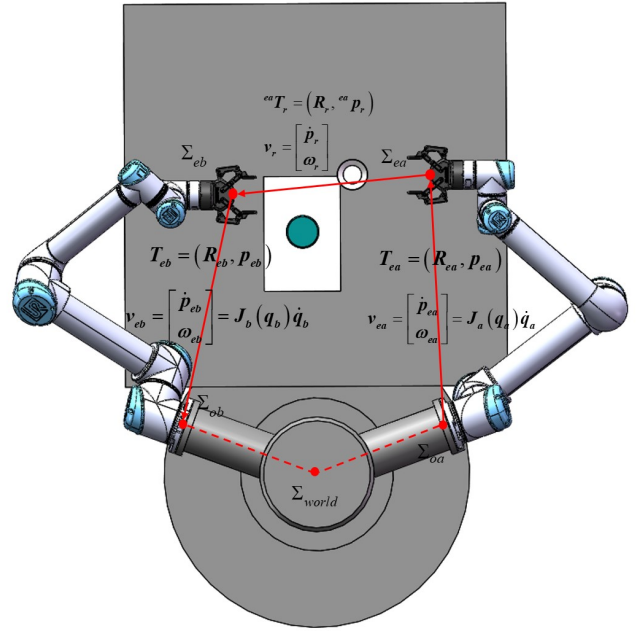


Fig. 1: Motion model coordinated by a dual-arm robot.

From the task point of view, the task-based formulation is defined by the absolute and relative motion variables of the cooperative system. The absolute and relative motion components can be derived from the end-effector coordinate frames as

$$\begin{cases} p_a = \frac{1}{2} (p_{ea} + p_{eb}) \\ R_a = R_{ea} R_{k_{a,b}} \left(\frac{1}{2} v_{a,b} \right) \end{cases} \quad (2)$$

where p_a is the position of the absolute coordinate frame Σ_a in the world frame Σ_{world} , R_a is the orientation of Σ_a with respect to Σ_{world} (absolute orientation), and $k_{a,b}$ and $v_{a,b}$ are extracted from the angle-axis representation of ${}^{ea}R_{eb} = R_{ea}^T R_{eb}$.

The relative position p_r and orientation R_r between two arms are defined as:

$$\begin{cases} p_r = p_{eb} - p_{ea} \\ R_r = R_{ea}^T R_{eb} = {}^{ea}R_{eb} \end{cases} \quad (3)$$

The absolute linear and angular velocities of the system are obtained as the time derivative of (2)

$$\begin{cases} \dot{p}_a = \frac{1}{2}(\dot{p}_{ea} + \dot{p}_{eb}) \\ \omega_a = \frac{1}{2}(\omega_{ea} + \omega_{eb}) \end{cases} \quad (4)$$

Similarly, the relative linear and angular velocities can be derived as

$$\begin{cases} \dot{p}_r = \dot{p}_{eb} - \dot{p}_{ea} \\ \omega_r = \omega_{eb} - \omega_{ea} \end{cases} \quad (5)$$

In the task space, the velocity of the end-effectors can be recovered via the absolute and relative motion:

$$\begin{bmatrix} v_{ea} \\ v_{eb} \end{bmatrix} = \begin{bmatrix} E_6 & -\frac{1}{2}E_6 \\ E_6 & \frac{1}{2}E_6 \end{bmatrix} \begin{bmatrix} v_a \\ v_r \end{bmatrix} \quad (6)$$

Assuming that motion of the object is known, the desired trajectories of the two arms can be derived by 3rd or 5th polynomial function. Thus, the desired motion of each end-effector can be obtained as

$$\begin{cases} v_{ea}^d = v_a^d - \frac{1}{2}v_r^d \\ v_{eb}^d = v_a^d + \frac{1}{2}v_r^d \end{cases} \quad (7)$$

where the right superscript $(\cdot)^d$ indicates the desired motion of the relevant variable.

It is clear from equation (7) that the cooperative task space is divided symmetrically between the two end-effectors: the prescribed absolute motion is executed equally by each arm, and the relative motion is divided evenly between them. The motion control law $\dot{x}_{ek}(t)$ of the end-effector in the task space with the error correction term can be written as

$$\begin{cases} \dot{x}_{ea}(t) = v_{ea}^d(t) + K_{ap}e_{ea}(t) + K_{ai} \int_0^T e_{ea}(t)dt \\ \dot{x}_{eb}(t) = v_{eb}^d(t) + K_{bp}e_{eb}(t) + K_{bi} \int_0^T e_{eb}(t)dt \end{cases} \quad (8)$$

where K_{kp} and K_{ki} are the 6×6 diagonal gain matrices, which take the form $k_p E$ and $k_i E$, respectively, where $k_p, k_i > 0$. Also, the configuration error $e_{ek}(t)$ can not be defined as $e_{ek}(t) = x_{ek}^d(t) - x_{ek}(t)$ as it does not make any sense to do the subtraction between two $SE(3)$. Instead, $e_{ek}(t)$ should refer to the twist which, if followed for a unit time, takes $x_{ek}(t)$ to $x_{ek}^d(t)$. The $se(3)$ representation of this twist can be expressed as $\log(R_{ek}^T(t)R_{ek}^d(t))$. Therefore, the configuration error is:

$$e_{ek}(t) = \begin{bmatrix} \log(R_{ek}^T(t)R_{ek}^d(t)) \\ p_{ek}^d(t) - p_{ek}(t) \end{bmatrix} \quad (9)$$

The error dynamics are governed by:

$$K_{kp}e_{ek}(t) + K_{ki} \int_0^T e_{ek}(t)dt = 0 \quad (10)$$

where a proper choice of K_{kp} and K_{ki} implies that $\lim_{t \rightarrow \infty} e_{ek}(t) = 0$.

Then, the desired angular velocity of each joint can be obtained by the inverse kinematics as:

$$\dot{q}_a^d = J_a^\dagger(q_a) \dot{x}_{ea} \quad (11)$$

$$\dot{q}_b^d = J_b^\dagger(q_b) \dot{x}_{eb} \quad (12)$$

where J_k^\dagger represents the generalized inverse of J_a .

In this manner, once the absolute and relative motions of the end-effectors are given in the task space, the joint angular velocities of the two arms can be quantitatively calculated accordingly. An advantage of using the absolute and relative strategies is that the dual-arm robotic system could be controlled without relying on the knowledge of the object or the environment.

B. Screw motion model

In the process of screwing the bottle cap, the end-effector of an arm performs a screw motion along the screw thread. A screw motion can be interpreted in terms of the screw axis S and a velocity $\dot{\theta}$ about that axis.

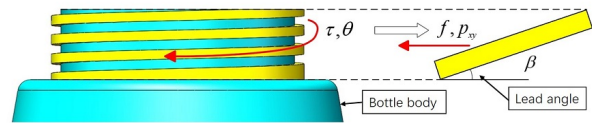


Fig. 2: Plane of screw thread

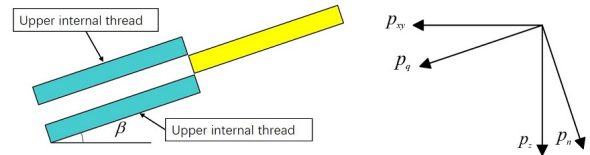


Fig. 3: Contact force between the internal and external screw threads

Fig. 2 shows the thread plane of the bottle and cap. In the developed thread plane, the rotary torque τ and rotary angle θ can be translated into the force f and the position p_{xy} along the screw axis S , respectively. Therefore, τ and θ are represented as:

$$f(t) = \frac{1}{r} \tau(t) \quad (13)$$

$$p_{xy}(t) = r\theta(t) \quad (14)$$

where r represents the radius of the screw.

We define the screw thread on the bottle as the external thread and the screw thread on the cap as the internal thread. When the cap is screwed, the external thread should slide into the internal thread, contacting with the lower internal thread or upper thread, and carry out the screw motion according to the thread track. Therefore, the contact model of the threads can be simplified as one external thread and two internal contacting threads. Fig. 3 shows the thread profile, where p_q represents the

rotational displacement along the thread, p_n represents the displacement of the thread orthogonal to the screw axis, p_t represents its displacement in the horizontal direction, p_z represents the displacement along the screw axis, i.e., the z -axis of the end-effector frame, and β represents the lead angle. The relationship between the screw motion of the bottle cap and the vertical motion along the direction of the axis can be expressed as:

$$\begin{bmatrix} p_q \\ p_n \end{bmatrix} = \begin{bmatrix} \cos \beta & \sin \beta \\ -\sin \beta & \cos \beta \end{bmatrix} \begin{bmatrix} p_{xy} \\ p_z \end{bmatrix} \quad (15)$$

Fig. 3 shows the contact force between the internal and external threads, where F_{ext} represents the pushing/pulling force along the screw axis, P_{env} is the friction force along the thread direction p_q , N_{env} represents the reaction force in the direction of p_n , and T_{ext} is the force in the p_t direction. During the motion of the bottle cap, T_{ext} and F_{ext} are the forces exerted by the gripper on the bottle cap, which generate P_{env} and N_{env} through the contact between the threads, respectively. Through the rotation matrix, the dynamic equation between the motion and force of the bottle cap can be expressed as:

$$M \begin{bmatrix} \ddot{p}_q \\ \ddot{p}_n \end{bmatrix} = \begin{bmatrix} \cos \beta & \sin \beta \\ -\sin \beta & \cos \beta \end{bmatrix} \begin{bmatrix} T_{ext} \\ F_{ext} \end{bmatrix} - \begin{bmatrix} P_{env} \\ N_{env} \end{bmatrix} \quad (16)$$

where M and \ddot{p} represent the mass and acceleration of the bottle cap, respectively. The forces P_{env} and N_{env} can be expressed as:

$$P_{env} = \mu N_{env} + D_p \dot{p}_q \quad (17)$$

$$N_{env} = K_n (p_n - p_{n0L}) + D_n \dot{p}_n \quad (18)$$

where μ , D , \dot{x} , K and p_{n0L} represent the dynamic friction coefficient, viscosity coefficient, velocity, stiffness, and position of the lower internal thread plane, respectively. When the cap and body of the bottle are tightened, no longer any relative motion exists between the threads, and the overall stiffness between the cap and body of the bottle increases. Therefore, at the moment of tightening, P_{env} needs to include additional stiffness terms.

$$P_{env} = \mu N_{env} + D_p \dot{p}_q + K_p (p_q - p_{q0}) \quad (19)$$

where p_{q0} represents the length of the thread. Through a force analysis, the reaction forces T_{env} and F_{env} in the p_t and p_z directions can be expressed as:

$$\begin{bmatrix} T_{env} \\ F_{env} \end{bmatrix} = \begin{bmatrix} \cos \beta & \sin \beta \\ -\sin \beta & \cos \beta \end{bmatrix} \begin{bmatrix} P_{env} \\ N_{env} \end{bmatrix} \quad (20)$$

To shorten the time of x_p reaching x_{p0} in equation (19), small P_{env} is desirable in equation (16). In equations (17) and (19), a decrease in N_{env} leads to small P_{env} . Moreover, N_{env} is calculated in terms of p_n . Therefore, p_n is required to be zero for small P_{env} . p_n in (15) can be rewritten as:

$$p_n = -p_{xy} \sin \beta + p_z \cos \beta \quad (21)$$

To control p_n as zero, the expected p_z can be written as:

$$p_z = p_{xy} \tan \beta = r \theta \tan \beta \quad (22)$$

Thus, along the screw axis, the relation between the expected linear displacement p_z^d and rotary angle θ^d can be described as:

$$p_z^d = r \theta^d \tan \beta \quad (23)$$

Differentiate both sides of equation (34), the expected linear and angular velocities in equation (2) should be constrained as:

$$v_z^d = r \omega_z^d \tan \beta \quad (24)$$

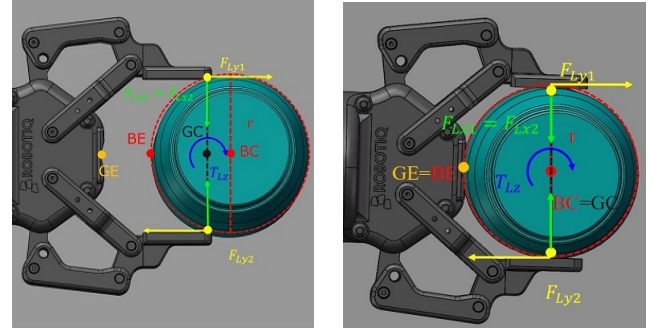
where v_z^d and ω^d are the desired relative linear and angular velocities along and about the screw axis S , respectively. Thus, the screw pitch can be defined as a constant as

$$h = \frac{v_z^d}{\omega_z^d} = r \tan \beta \quad (25)$$

III. Contact State Identification

The precise online identification of contact states is necessary for the successful execution of a fine motion. Taking the bottle screwing task as an example, the model of the contact state identification is discussed.

In Fig. 4, the contact state between the fingers and the bottle body is analyzed. If the center of the gripper GE does not contact with the edge of the bottle body BE , the force closure will be broken, and the grasp is not stable, as shown in Fig. 4(a). In this case, the gripper will exert an additional torque T_{Lz} on the bottle body, which may cause an unexpected movement or uncertainty, resulting in failure of the task. The expected contact state is shown in Fig. 4(b), where the gripper center and the bottle body center coincide with each other.



(a) The center of the gripper does not coincide with the center of the bottle body. (b) The center of the gripper coincides with the center of the bottle body.

Fig. 4: Force analysis of steady gripping of the bottle body

One way to guarantee the grasp maintenance is to carry out edge detection. As shown in Fig. 5(a), the finger of the gripper can be used to detect the edge of the cap. When a certain force feedback is read, the position of the end-effector is recorded. After getting three feature points, the center of the cap can be calculated, as shown in Fig. 5(b).

To calculate the center point CC , the intersection points of S_1 and l_1 as well as l_2 and S_2 are determined as

$$x_{ic} = \frac{x_1 + x_{i+1}}{2}, y_{ic} = \frac{y_1 + y_{i+1}}{2} \text{ with } i = 1, 2. \quad (26)$$

A line can be described as $\Delta y/\Delta x = \text{const}$, thus:

$$\frac{(y - y_{ic})}{(x - x_{ic})} = \frac{(y_1 - y_{i+1})}{(x_1 - x_{i+1})} = \frac{-1}{k_i} \text{ with } i = 1, 2 \quad (27)$$

Thus, the bisectors, which are perpendicular to the secant and passing through (x_{1c}, y_{1c}) and (x_{2c}, y_{2c}) , can be described as:

$$l_i : (y - y_{ic}) = k_i(x - x_{ic}) \text{ with } i = 1, 2 \quad (28)$$

The intersection point of the two bisectors is the desired center of the cap. Hence, equalizing lines l_1 and l_2 , we obtain the coordinates (x_m, y_m) of the center point CC .

$$x_m = \frac{-y_{1c} + y_{2c} + k_1x_{1c} - k_2x_{2c}}{k_1 - k_2} \quad (29)$$

$$y_m = y_{1c} + k_1(x_m - x_{1c})$$

The radius r can be expressed as

$$r = \sqrt{(x_i - x_m)^2 + (y_i - y_m)^2} \text{ with } i = 1, 2 \text{ or } 3. \quad (30)$$

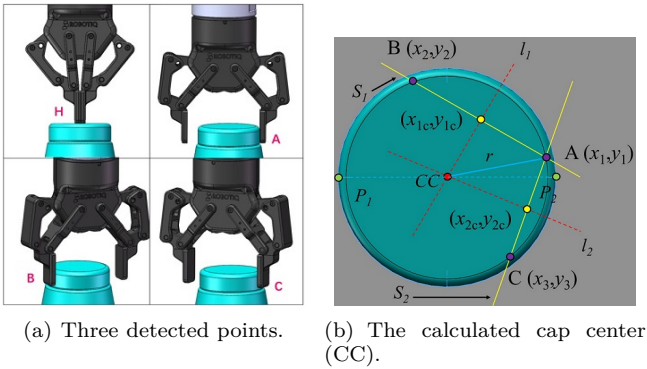


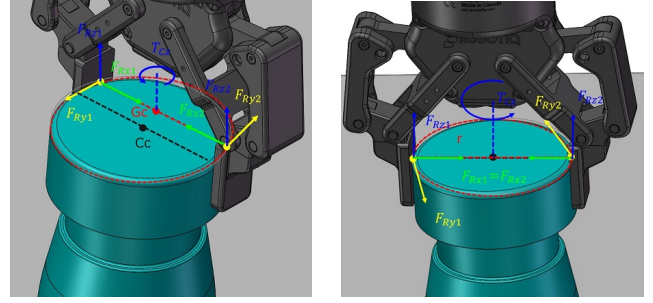
Fig. 5: Geometrical center of the bottle cap.

Therefore, the position and attitude of the gripper can be adjusted to grasp the cap through the straight line passing through the center of the cap.

In Fig. 6(a), the center of the gripper GC does not coincide with that of the cap CC . When the gripper screws the cap, an undesirable contact sliding may take place. Through the object detection method, the grasp maintenance can be guaranteed as shown in Fig. 6(b). It is partial form closure and force closure.

These force/torque constraints in equation (31) can be used to determine the contact state between the cap and body of the bottle, which is of great significance for planning of online fine motion and effective reduction of uncertainties. The torque T_{Cz} goes through the center of the cap. T_{Cz} should have upper and lower bounds as expressed in equation (31). When T_{Cz} is less than T_{min} , sliding occurs between the fingertip and the cap. When T_{Cz} is bigger than T_{max} , the bottle cap and the bottle body get stuck, requiring to unscrew the cap in the opposite direction and then to readjust.

$$T_{min} \leq |T_{Cz}| \leq T_{max} \quad (31)$$



(a) The gripper center does not coincide with the cap center. (b) The gripper center coincides with the cap center.

Fig. 6: Force analysis between the gripper and the bottle cap.

By introducing the techniques of contact state identification and force/torque constraints, the motion uncertainties could be reduced significantly.

IV. Task-based Motion Planning with Compliance Control

The motion of the bottle screw has to tackle some uncertainties to make the task successful. Therefore, the motion planning for the manipulation task can be divided into two layers: gross motion planning and fine motion planning.

A. Gross motion planning

In the bottle screwing task, the objective of the gross motion planning is to address a collision-free motion planning problem in a changing environment. Let $q_{init} \in C_{free}$ be an initial joint configuration and $q_{goal} \in C_{free}$ be a goal joint configuration, where C_{free} denotes the collision-free configuration. There should be safe distances between the two arms and the environment. Given the desired poses x_{ea}^d and x_{eb}^d of the two end-effectors according to the bottle pose, the desired joint configuration q^d can be calculated using inverse kinematics. The environment is not static, but its changes over time can be predicted, i.e., $env(t)$ is given. A task-time configuration space $S \subset C \times R$ is created. For given initial and goal configuration in the task-time configuration space, $s_0 = \langle q_0^d, 0 \rangle$ and $s_T = \langle q_T^d, T \rangle$, respectively, the gross motion planning problem can be defined as:

$$q_{[0:T]} = \text{GrossMotionPlanning}(s_0, s_T, env(t)) \quad (32)$$

$$s.t. \forall t \in [0 : T] : \text{Collision-Free}(q_t, env(t))$$

where Collision-Free indicates the configuration space where the two arms would not collide with each other or the environment.

B. Fine Compliance Control

A fine compliance control in a domain of robotics is restricted to a small-scale space and contacts between the interacting objects, e.g., opening a can, driving a screw,

or installing a fuse or a light bulb. In order to perform this kind of tasks, the robot has to control the position of the object along the screw axis and contact forces between the two parts to avoid jamming. In our work, the task of screwing a cap requires that the position and force control are seamlessly integrated.

The position-based impedance control translates the force/torque error of the end-effector to the input correction of position or attitude. The differential equation of the impedance control can be described as:

$$M\Delta\ddot{x}_{eb} + B\Delta\dot{x}_{eb} + K\Delta x_{eb} = \Delta F_{eb} \quad (33)$$

where M , B and K represent the inertia, damping, and stiffness parameter, $\Delta x_{eb} = x_{eb} - x_{eb}^d$ is the position deviation, x_{eb} and x_{eb}^d are the actual and desired relative motions of the slave arm, respectively; and ΔF_{eb} is the general force deviation. When the force deviation ΔF_{eb} is detected by the force/torque sensor, the position adjustment can be obtained by Laplace transform as:

$$\Delta x_{eb}(s) = \frac{\Delta F_{eb}(s)}{Ms^2 + Bs + K} \quad (34)$$

The impedance Y is defined by the transfer function from the force perturbations to positions as

$$Y_{eb}(s) \triangleq \frac{\Delta x_{eb}(s)}{\Delta F_{eb}(s)} \quad (35)$$

A good fine motion controller is characterized by a low impedance as $\Delta x_{eb} = Y_{eb}\Delta F_{eb}$, and a small Y_{eb} implies that force perturbations produce only small position perturbations. Thus, the controller can guarantee the accuracy of the task execution.

Finally, the fine compliance control of the slave arm can be realized by directly adding Δx_{eb} to \dot{x}_{eb}^d as

$$\dot{q}_b^d = J_b^\dagger (\dot{x}_{eb} + \Delta x_{eb}) \quad (36)$$

where the linear and angular velocities of \dot{x}_{eb} subject to the constraint equation (24).

Fig. 7 shows the control structure of the bottle screw manipulation by a dual-arm robot.

V. Experimental study

In order to demonstrate the effectiveness of the proposed method, a dual-arm robot system was built up to carry out the bottle screwing task. The dual-arm robot consisted of two 6-DoF UR5 arms, both equipped with Robotiq force/torque sensors. The details about the UR5 and force torque sensor could be found in [21]. The control programs were developed through ROS with Ubuntu 16.04. The master arm gripped the bottle body and the slave one manipulated the bottle cap. Fig. 8 shows the key frames of the task manipulation.

In the bottle screw manipulation progress, the interaction forces and torques of the two arms are shown in Fig. 9–Fig. 12, respectively. Because there existed kinematic uncertainties, the two arms interacted with each other during the opening and screwing process, causing the forces and torques fluctuated within the safety threshold.

The fluctuation of the master arm is from the gross motion, as shown in Fig. 13 and Fig. 14, from which we can find that the task-based control strategy is feasible for the dual-arm manipulation to complete a bottle screw task.

The whole process is divided into four phases:

- 1) Grasping: In the grasping phase, the main objective is to generate a collision-free trajectory and grasp the bottle body and cap stably. The whole process lasts 52s, which is divided into two stages: gripping the bottle body (0 – 27s) and gripping the bottle cap (27s – 52s). In the first stage, P_1 is the initial configuration. At $t = 12s$, the master arm reaches the pre-contact configuration, where the object detection by the use of a force/torque sensor is applied to compensate for the position uncertainty of the bottle. When the sensed force along the z -axis is bigger than the threshold 2N (2.12N in Fig. 9), the gripper closes to complete the grasping of the bottle body. In order to demonstrate that the bottle cap is fasten and there is no leakage, the bottle is rotated 60 degree. In the second stage, the slave arm reaches a relative posture through the preset relative position and attitude of the master arm. The height of the bottle cap is detected, and the cap center is calculated by the feature points. Then, the optimal gripping position is determined, where the center of the fingertips coincides with the geometric center of the bottle cap.
- 2) Opening: The opening process lasts for about 20s, from 52s to 72s. The slave arm performs a screw motion, as shown in P_2 . During the opening process, the maximum torque is 2.2Nm, which is less than the preset constraint of 4Nm in equation (31). If this constraint is violated, the bottle cap probably gets stuck, and the gripper needs to unscrew the cap. Otherwise, the position control will be executed. However, due to the interaction between the cap and body of the bottle, there are contact forces and torques, as shown in Fig. 9–Fig. 12, respectively. When the pulling force in the end-effector of the slave arm returns to neighborhood of zero, the cap is opened completely and reaches the state in P_3 .
- 3) Pouring water: After opening the bottle cap, the robot pours water from the bottle into a cup, and then returns to the original position, respectively. In this process, the slave arm remains static. The force/torque sensor on the end-effector is required to monitor whether a collision occurs. After pouring water, the force/torque sensor is calibrated due to the change of the center of gravity of the bottle.
- 4) Screwing fasten the bottle cap: Screwing the bottle cap back onto the body starts at 95s. Firstly, the slave arm with the cap moves down until the contact force becomes bigger than the force threshold 4N (4.33N in Fig. 11). Then, the robot arm conducts click detection in P_4 . When a sudden change in the

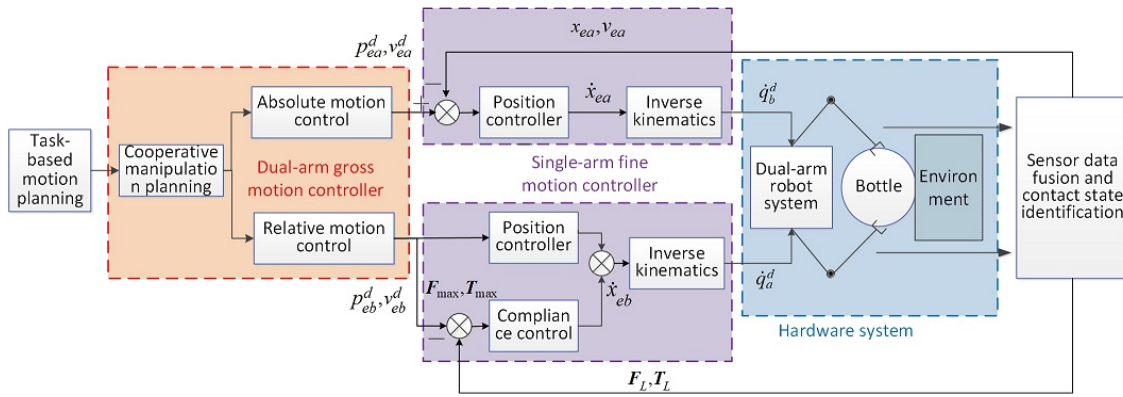


Fig. 7: Overview of the control pipeline for the bottle screwing task.

contact force occurs ($t = 109.8s, 10.12N$, as shown in Fig. 11), the robot arm starts to fasten the bottle cap. During the screwing process, the pushing force along the z -axis is maintained within $10N$. When the torque around the z -axis exceeds $2Nm$ and the pulling force is bigger than $15N$, the bottle cap is proved to be tightened. Then, the slave arm returns to the original position, the master arm rotates to prove that the bottle cap is tightened and there is no leakage. Finally, the robot arm puts the bottle on the table and goes back to the original configuration.

To verify the robustness of the control strategy, another bottle with different size and type is also manipulated, as shown in Fig. 15. The size of the bottle, number of threads, thread pitch and material are totally different from those of the previous one. The success of this experiment proves that the proposed control method is able to handle the bounded uncertainty owing to the unmodel kinematics and dynamics of the robot and object.

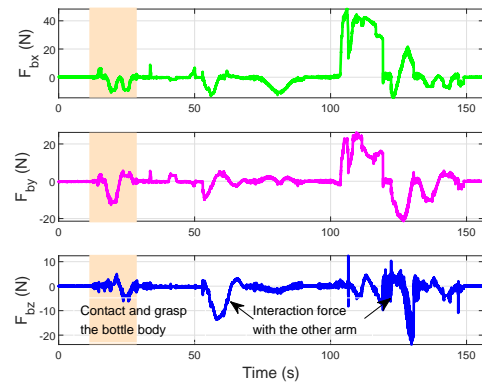


Fig. 9: The sensed force of the master arm.

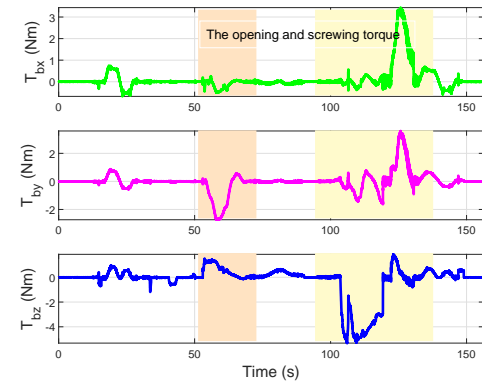
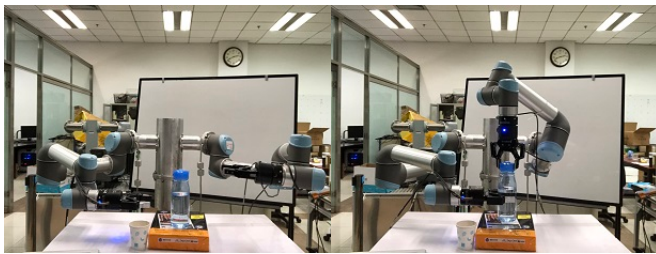
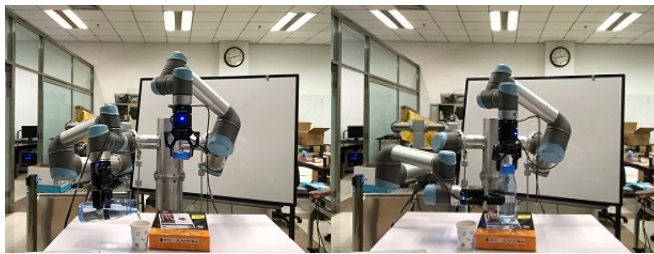


Fig. 10: The sensed torque of the master arm.



(a) P_1 .

(b) P_2 .



(c) P_3 .

(d) P_4 .

Fig. 8: The key frames of the proposed manipulation planning strategy for the bottle screwing task.

VI. Conclusion

In this paper, we propose a task-based compliance control scheme for a bottle screw manipulation, which is inspired by the human behavior. With the consideration of uncertainties, a hierarchical control strategy is provided. The gross motion planning is conducted by the master arm to carry out the absolute motion, while the fine motion planning is designed to deal with uncertainties caused by the relative motion. Furthermore, a position-based impedance control scheme is integrated into the

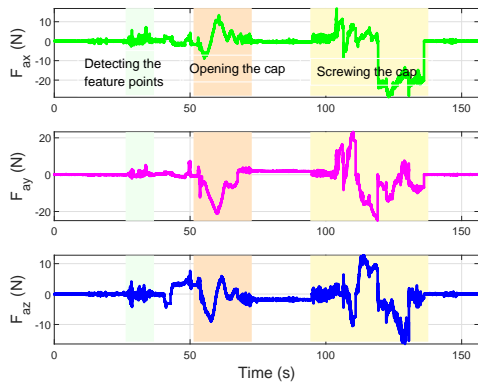


Fig. 11: The sensed force of the slave arm.

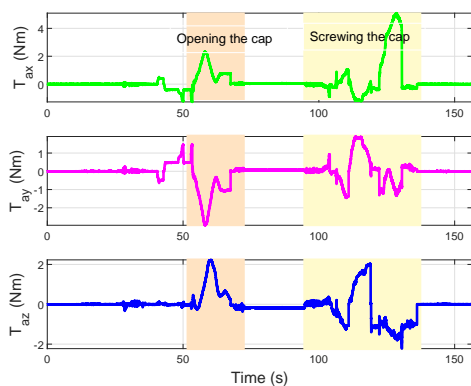


Fig. 12: The sensed torque of the slave arm.

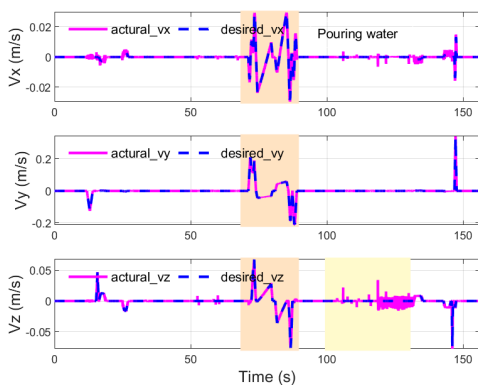


Fig. 13: The linear velocity of the master arm.

fine motion planning on the slave arm. The proposed compliance control scheme has better performance gain to avoid the occurrence of jamming by the fine compliant control. Experiments are conducted with two different bottles. From the experimental results, we can conclude that the proposed task-based compliance control scheme is applicable and robust enough for a dual-arm robot to complete a complex task. In future work, the artificial intelligent skill and vision recognition will be taken into account to handle more complex tasks.

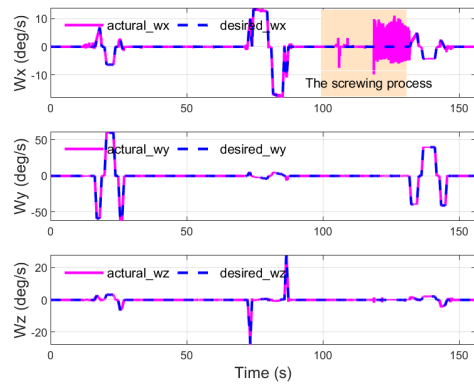


Fig. 14: The angular velocity of the master arm.

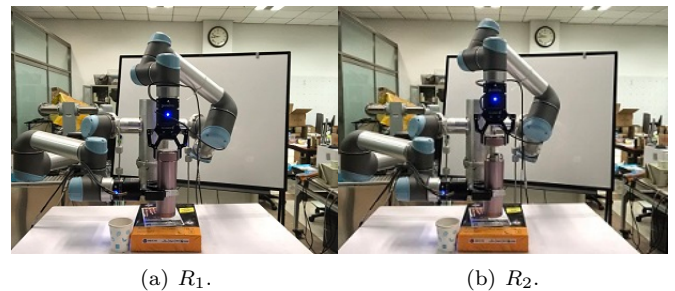


Fig. 15: The key frames of the proposed manipulation planning strategy for the bottle screwing task.

References

- [1] L. Han, W. Xu, B. Li, and P. Kang, "Collision detection and coordinated compliance control for a dual-arm robot without force/torque sensing based on momentum observer," *IEEE/ASME Transactions on Mechatronics*, vol. 24, no. 5, pp. 2261–2272, 2019.
- [2] B. Xiao, S. Yin, and O. Kaynak, "Tracking control of robotic manipulators with uncertain kinematics and dynamics," *IEEE Transactions on Industrial Electronics*, vol. 63, no. 10, pp. 6439–6449, 2016.
- [3] F. Shen, F. Qin, Z. Zhang, D. Xu, J. Zhang, and W. Wu, "Automated pose measurement method based on multivision and sensor collaboration for slice microdevice," *IEEE Transactions on Industrial Electronics*, vol. 68, no. 1, pp. 488–498, 2021.
- [4] J. Su, C. Liu, and R. Li, "Robot precision assembly combining with passive and active compliant motions," *IEEE Transactions on Industrial Electronics*, vol. 69, no. 8, pp. 8157–8167, 2021.
- [5] S. Liu, D. Xu, F. Liu, D. Zhang, and Z. Zhang, "Relative pose estimation for alignment of long cylindrical components based on microscopic vision," *IEEE Transactions on Mechatronics*, vol. 21, no. 3, pp. 1388–1398, 2016.
- [6] S. Liu, D. Xu, D. Zhang, and Z. Zhang, "High precision automatic assembly based on microscopic vision and force information," *IEEE Transactions on Automation Science and Engineering*, vol. 13, no. 1, pp. 382–393, 2016.
- [7] S. Liu, Y. F. Li, D. P. Xing, D. Xu, and H. Su, "An efficient insertion control method for precision assembly of cylindrical components," *IEEE Transactions on Industrial Electronics*, vol. 64, no. 12, pp. 9355–9365, 2017.
- [8] H. Park, J. Park, D. H. Lee, J. H. Park, M. H. Baeg, and J. H. Bae, "Compliance-based robotic peg-in-hole assembly strategy without force feedback," *IEEE Transactions on Industrial Electronics*, vol. 64, no. 8, pp. 6299–6309, 2017.
- [9] C. Jiao, L. Yu, X. Su, Y. Wen, and X. Dai, "Adaptive hybrid impedance control for dual-arm cooperative manipulation with object uncertainties," *Automatica*, vol. 140, June, 2022.

- [10] J. Xu, Z. Hou, W. Wang, B. Xu, K. Zhang, and K. Chen, "Feedback deep deterministic policy gradient with fuzzy reward for robotic multiple peg-in-hole assembly tasks," *IEEE Transactions on Industrial Informatics*, vol. 15, no. 3, pp. 1658–1667, 2019.
- [11] V. Chawda and G. Niemeyer, "Toward torque control of a kuka lbr iiwa for physical human-robot interaction," *IEEE/RSJ International Conference on Intelligent Robots and Systems*, pp. 6387–6392, Vancouver, BC, Canada, September 2017.
- [12] M. Bednarczyk, H. Omran, and B. Bayle, "Model predictive impedance control," *IEEE International Conference on Robotics and Automation*, pp. 4702–4708, Paris, France, May 2020.
- [13] Y. Ren, Z. Chen, Y. Liu, Y. Gu, M. Jin, and H. Liu, "Adaptive hybrid position/force control of dual-arm cooperative manipulators with uncertain dynamics and closed-chain kinematics," *Journal of the Franklin Institute*, vol. 354, no. 17, pp. 7767–7793, 2017.
- [14] L. Su, C. Wang, H. Chang, Y. Yang, and W. Assawinchaichote, "Event-triggered sliding mode control of networked control systems with Markovian jump parameters," *Automatica*, vol. 112, pp. 109405, 2021.
- [15] X. Su, X. Liu, and Y. Song, "Event-triggered sliding mode control for multi-area power systems," *IEEE Transactions on Industrial Electronics*, vol. 64, no. 8, pp. 6732–6741, 2017.
- [16] Y. Sun, Y. Gao, Y. Zhao et al., "Neural network-based tracking control of uncertain robotic systems: predefined-time nonsingular terminal sliding-mode approach," *IEEE Transactions on Industrial Electronics*, vol. 69, no. 10, pp. 10510–10520, 2022.
- [17] Y. Sun, J. Liu, Y. Gao, Z. Liu, and Y. Zhao, "Adaptive neural tracking control for manipulators with prescribed performance under input saturation," *IEEE/ASME Transactions on Mechatronics*, pp. 1–10, 2022.
- [18] Z. Liu, O. Zhang, Y. Gao, Y. Zhao, Y. Sun, and J. Liu, "Adaptive neural network-based fixed-time control for trajectory tracking of robotic systems," *IEEE Transactions on Circuits and Systems II: Express Briefs*, pp. 1–1, 2022.
- [19] L. Wu, J. Liu, S. Vazquez, and S. K. Mazumder, "Sliding mode control in power converters and drives: a review," *IEEE/CAA Journal of Automatica Sinica*, vol. 9, no. 3, pp. 392–406, 2022.
- [20] H. Lee and H. J. Kim, "Constraint-based cooperative control of multiple aerial manipulators for handling an unknown payload," *IEEE Transactions on Industrial Informatics*, vol. 13, no. 6, pp. 2780–2790, 2017.
- [21] P. M. Kebria, S. Alwais, H. Abdi, and S. Nahavandi, "Kinematic and dynamic modelling of ur5 manipulator," *IEEE International Conference on Systems, Man, and Cybernetics*, pp. 4229–4234, Budapest, Hungary, October 2016.



Chunting Jiao received the B.S. degree in Automation from Xi'an Jiaotong University, Shaanxi, China, in 2012; the M.E. degree in Control science and project from Xi'an Jiaotong University, Shaanxi, China, in 2015; and the Ph.D. degree in Control Science and Engineering from Tsinghua University, Beijing, China in 2020. He is currently an assistant researcher with the College of Automation, Chongqing University, Chongqing, China. His current research interests include intelligent control systems, robot manipulation, and motion planning.



Lin Zhang was born in Chongqing, China, in 1998. She received the B.S. degree in Automation from Chongqing University, Chongqing, China, in 2020. She is currently working toward the PhD degree in Control Theory and Control Engineering in the College of Automation from Chongqing University, Chongqing, China. Her research interests include multi-robot systems, motion control and artificial intelligence in robotics.



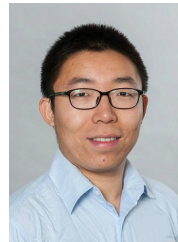
Xiaojie Su received the PhD degree in Control Theory and Control Engineering from Harbin Institute of Technology, China in 2013. He is currently a professor and dean with the College of Automation, Chongqing University, Chongqing, China. His current research interests include intelligent control systems and application of intelligent robot control. He has published 3 research monographs and more than 100 research papers in international referred journals.

Prof. Su is the Founding Chair, IEEE Beijing Section, Systems, Man, and Cybernetics and Robotics and Automation Joint Societies Chapter (CH10994). He currently serves as an Associate Editor for a number of journals, including *IEEE Transactions on Artificial Intelligence*, *IEEE Transactions on Fuzzy Systems*, *IEEE Transactions on Systems, Man, and Cybernetics: Systems* and so on. He was named to the 2017–2022 Highly Cited Researchers list, Clarivate Analytics.



Jiangshuai Huang received the B.Eng. and M.Sc. degrees from the School of Automation, Huazhong University of Science and Technology, Wuhan, China, in July 2007 and August 2009, respectively, and the Ph.D. degree from Nanyang Technological University, Singapore, in 2015.

He is currently with the School of Automation, Chongqing University, Chongqing, China. His research interests include adaptive control, nonlinear systems control, underactuated mechanical system control, and multiagent system control. His current interests include control theory and control engineering, fuzzy control, and machine learning and its application.



Zhenshan Bing received his doctorate degree in Computer Science from the Technical University of Munich, Germany, in 2019. He received his B.S. degree in Mechanical Design Manufacturing and Automation from Harbin Institute of Technology, China, in 2013, and his M.Eng. degree in Mechanical Engineering in 2015, at the same university. Dr. Bing is currently a postdoctoral researcher with Informatics 6, Technical University of Munich, Munich, Germany. His research investigates

the snake-like robot which is controlled by artificial neural networks and its related applications.



Alois Knoll (Senior Member) received his diploma (M.Sc.) degree in Electrical/Communications Engineering from the University of Stuttgart, Germany, in 1985 and his Ph.D. (summa cum laude) in Computer Science from Technical University of Berlin, Germany, in 1988. He served on the faculty of the Computer Science department at TU Berlin until 1993.

He joined the University of Bielefeld, Germany as a full professor and served as the director of the Technical Informatics research group until 2001. Since 2001, he has been a professor at the Department of Informatics, Technical University of Munich (TUM), Germany. He was also on the board of directors of the Central Institute of Medical Technology at TUM (IMETUM). From 2004 to 2006, he was Executive Director of the Institute of Computer Science at TUM. Between 2007 and 2009, he was a member of the EU's highest advisory board on information technology, ISTAG, the Information Society Technology Advisory Group, and a member of its subgroup on Future and Emerging Technologies (FET). In this capacity, he was actively involved in developing the concept of the EU's FET Flagship projects. His research interests include cognitive, medical and sensor-based robotics, multi-agent systems, data fusion, adaptive systems, multimedia information retrieval, model-driven development of embedded systems with applications to automotive software and electric transportation, as well as simulation systems for robotics and traffic.